2.3 SMALL SCALE SIMULATION AND LIDAR VALIDATION OF A SHALLOW LAND BREEZE FRONT

Gijs de Boer*, Gregory J. Tripoli, and Edwin W. Eloranta
University of Wisconsin – Madison, Madison, Wisconsin

1. INTRODUCTION

As part of the Lake-Induced Convection Experiments (Lake-ICE) (Kristovich et al., 2000), on December 21, 1997 the University of Wisconsin Volume Imaging Lidar (UW-VIL) observed a persistent, shallow lake breeze circulation over western Lake Michigan. In this study, an attempt is made to simulate this small-scale flow using the University of Wisconsin Non-Hydrostatic Modeling System (UW-NMS) (Tripoli, 1992). Previous attempts at simulation of events at similar scales (Mayor, 2001; Moeng and Sullivan, 1994) have focused mainly around large eddy simulations (LES). Non-LES efforts towards simulating similar structures have typically had insufficient resolution to accurately simulate the small-scale processes occurring within the planetary boundary layer (Alpert and Neumann, 1983; Ballentine, 1982). With advances in computer technology however, nested, non-LES simulations have the ability to become more advanced through the utilization of larger high-resolution domains.

The land breeze case chosen for this study represents the type of structure that, so far, has not been simulated at a high resolution, while still including the effects of large-scale atmospheric features. As mentioned above several efforts have been made at simulation of the land breeze, but many of these attempts have fallen short in reproducing some of the dynamical aspects of the circulation. The studies by Alpert and Neumann, and Ballentine focus more on the simulation of the occurrence of the land breeze, rather than the structure of the flow in and around the circulation. Sha, et al. (1991) completed a study that described, at a more in depth level, the structure of the circulation, the nose of the circulation, as well as what effects the circulation had on the rest of the surrounding atmosphere. More specifically, the land breeze was treated as a gravity current, with the head of the current investigated as a possible source for Kelvin-Helmholtz type billows formed in its wake.

Another important issue in the simulation of these structures has been the validation of model output. Until recently, most validation was done using data gathered from point measurements taken either by instruments set up in a grid in the area of interest (Shafran et al., 1998; Ohara et al., 1989) or by airplane based instrumentation (Agee and Hart, 1990). Advances in several remote-sensing techniques have dramatically improved data collection for boundary layer flows. Utilized instruments include dual Doppler radar (Atkins et al., 1995), synthetic aperture radar (SAR) (Winstead and Mourad, 2000), and lidar (Mayor et al., 2003; Fast and Darby, 2004). The ability of lidar systems to detect clear-air atmospheric structures not readily observed with other platforms, along with the fact that observations of a large volume of air can be made in a couple of minutes makes this a very enticing tool for boundary layer investigations. Mayor et al. (2003) employed lidar data collected with the UW-VIL to validate his LES, utilizing a virtual scattering parameter, as well as cross-correlation techniques in order to attempt direct comparison between the data and simulations. This study will utilize a similar virtual scattering parameter, along with visual comparison of flow features such as boundary layer depth, land breeze depth, land breeze head depth, horizontal extent of the land breeze, wind speed and direction, and the structure and size of convective structures in the flow outside of the land breeze for analysis of the accuracy of the numerical simulation.

2. THE UNIVERSITY OF WISCONSIN VOLUME IMAGING LIDAR (UW-VIL)

The UW-VIL is an elastic backscatter lidar that has evolved over the past several decades. It was

* *Corresponding author address*: Gijs de Boer, University of Wisconsin – Madison, Department of Atmospheric and Oceanic Sciences, 1225 West Dayton Street, Madison, WI 53706; e-mail: gdeboer@wisc.edu

designed for four-dimensional data collection of the atmospheric boundary layer. The most recent version came together in 1995, when an SGI workstation for data processing was added, along with a high power Infinity Coherent 40-100 Nd:YAG laser. The laser has several important characteristics, including a diode pumped seed laser and two flash lamp pumped amplification stages. Additionally, it incorporates a phase conjugate mirror in order to protect the quality of the wave front from distortion when passing through the high-heat areas of the amplifier.

The system transmitter operates at 1064 nm, with an average power of 40 watts, and a 100 Hz repetition rate. The receiver utilizes a 0.5 m telescope set up in a cassegrain configuration, with a 1 nm optical bandwidth. This allows for 15 m range resolution and a maximum angular scan rate of around 20 degrees per second. The combination of the powerful laser and the large telescope allows detection of aerosol structures up to a range of 30 km in a clear atmosphere.

Since molecular scattering is relatively small at 1064 nm, the backscatter is largely dependent upon the aerosol distribution in the atmosphere, and the range squared dependence of the backscatter. Because of this sensitivity, differing aerosol concentrations, as often found inside convective boundary layer structures are detected very easily. In addition to this, in the land breeze case, there is a strong relative humidity gradient due to the differences in temperature between the cold offshore land breeze and the warmer flow arriving onshore from over the Lake Michigan surface. Since atmospheric aerosols tend to swell in high relative humidity, this further enhances the contrast between the land breeze circulation and the prevailing, synoptically forced flow.

For boundary layer applications, three main scan strategies are employed. The first involves keeping the azimuth angle constant while scanning between elevation angles and is known as a Range-Height Indicator (RHI). The second is a similar technique, with the exception that after each RHI is completed, the azimuth changes, creating an RHI volume scan. The third scanning strategy utilized is a plane parallel indicator scan (PPI) in which the elevation angle is held constant, but the azimuthal angle is changed. Constant altitude PPIs (CAPPIs) are created through interpolation in order to attempt to negate the angle at which the beam exits the transmitter, relative to the earth.

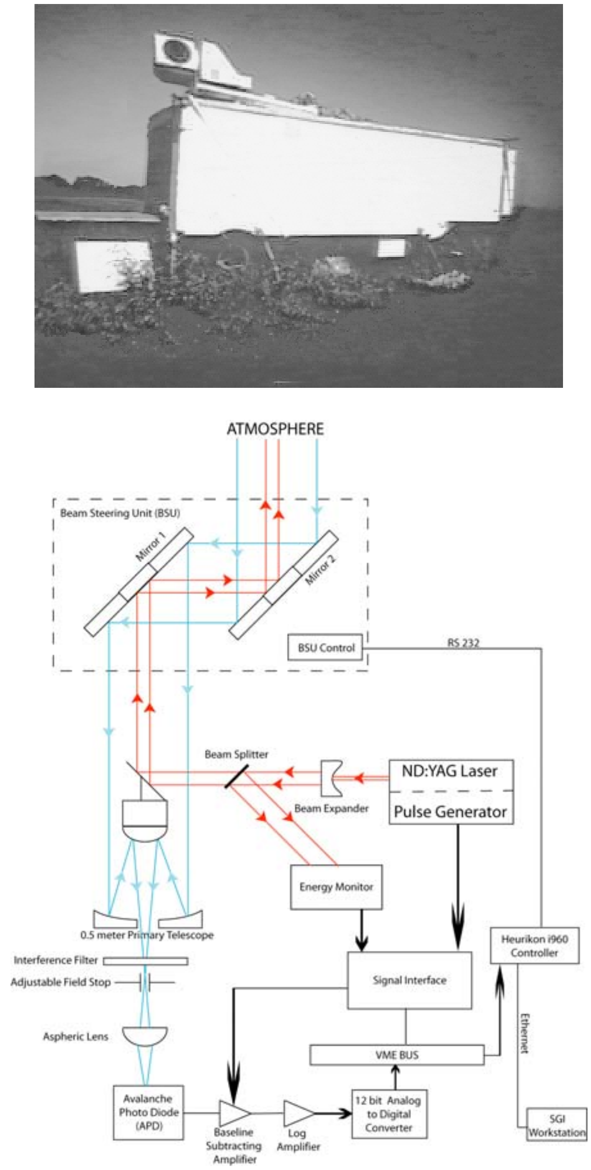

Figure 1: An image (top) and schematic (bottom) of the UW-VIL.

3. THE UNIVERSITY OF WISCONSIN NON-HYDROSTATIC MODELING SYSTEM (UW-NMS)

The simulations run in this study used the UW-NMS. This model has several features making it attractive for this sort of simulation. The first of these features is a two-way grid nesting system. Through this, higher resolutions needed for these simulations can be attained, and feedback from both the large and small scales affects the flow at other scales. Another attractive feature is that this model is non-hydrostatic. Since the vertical

Figure 2: A map showing the location of Sheboygan, Wisconsin (top) and the nested grid arrangement for simulation 'A' (bottom). Grid 6 is focused just off of Sheboygan Point for this simulation.

momentum equation is solved, convective structures in the flow can be replicated. Topography is handled using a variably stepped system, meaning that although a step coordinate system is used, the traditional handicap of not being able to represent subtle topographical changes is not a factor. This is because grid boxes containing topography can be partially filled based on the height of the topography at that location. The centers of those grid boxes are then adjusted to represent the center of the above ground volume. For these simulations, a high-resolution representation of Wisconsin's topography was employed, featuring 100 m resolution.

These particular simulations included six nested grids, the largest of which covered approximately two-thirds of the continental United States, and the smallest of which utilized 32 m resolution. Twenty meter spacing was used vertically for the first 15 grid cells (up to 300 m) at which point, the resolution was stretched by 120%, with a maximum step of 750 m. Fifty vertical points at this resolution allowed the simulation to cover up to around 15 km. This resolution allowed us to compare structures seen in the simulations with those detected by the lidar. Figure 2 shows

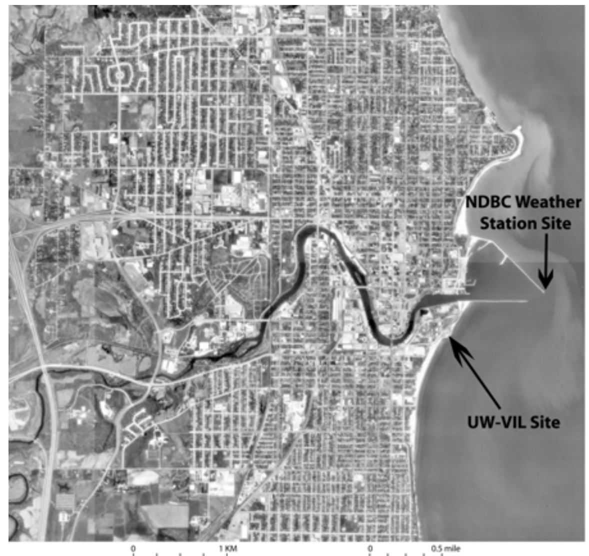

Figure 3: Satellite image of Sheboygan Point, indicating the locations of the UW-VIL and the NDBC site. (Image courtesy of the USGS)

the location of the nested grids, as used for the smaller of the two simulations discussed here.

4. DECEMBER 21, 1997: LAKE-ICE

During the Lake Induced Convection Experiments (Lake-ICE, winter of 1997-1998), the UW-VIL was located on the southern part of Sheboygan Point in order to capture the convective structure of the boundary layer during cold air outbreaks. Additional instruments taking part in the study included two National Centers for Atmospheric Research (NCAR) aircraft, three NCAR Integrated Sounding Systems (ISS) the Pennsylvania State University Cloud Observing System (PSU-COS), several National Weather Service WSR-88D radar sites, and satellite based SAR imagery. In addition to these instruments, the National Data Buoy Center (NDBC) has a data recording station within 1 km of the lidar site. An image showing Sheboygan Point and the location of the lidar and the NDBC site is shown in figure 3.

On December 21, 1997 the scientists on location at the VIL site noticed the presence of a land breeze by the fact that the smokestack plumes from the power plant on the shoreline were blowing opposite the direction of surface winds. A lake/land temperature difference of approximately3-5° C was in place (figure 4), with a weak westerly breeze observed at the lidar site.

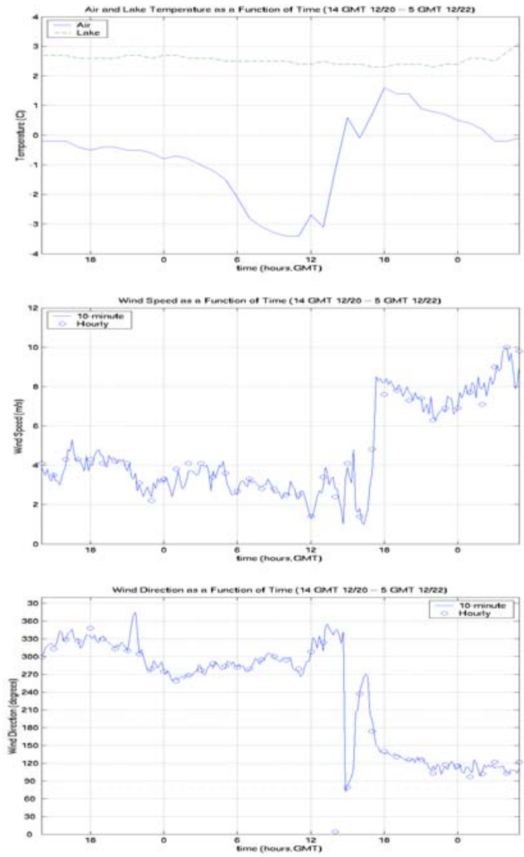

Figure 4: Hourly temperature (top), wind speed (middle), and wind direction (bottom) data taken at the NDBC site at Sheboygan Point. The time scale ranges from 14 GMT 20 December to 5 GMT 22 December.

4.1 *Lidar Data*

All three of the previously described scanning patterns were utilized in order to capture the land breeze, with almost three hours of RHI volume scans, an hour and a half or so of PPI scanning, about 20 minutes of an RHI scan at the end of data collection. Figure 5 shows a time progression of the RHI volume scans taken on the date. In this image, the land breeze is visible as the area of stronger scattering on the left side of the viewed area. The set of CAPPIs at the bottom of these images give a good indication of the shallow nature of this circulation, with only the head of the land breeze showing up at 160 m. Also, the horizontal extent of the circulation can be determined from the CAPPIs more effectively than the RHI scan at the top, since the RHI is taken at some angle to the shoreline, in this case 144.5°. Although originally at around 7-8 km offshore, the land breeze front appears very clearly at around 3-4 km later in the collection period (middle and bottom images, figure 5). Additionally, the top of the boundary layer can be seen in the RHIs in this image as a undulating feature around 700-800 m. Another thing to note is the recession of the land breeze toward the shoreline as the large-scale winds increase in magnitude during the day. With this increase, the land breeze becomes much shallower and the intersection between the flows is much better defined. The nose of the circulation appears to be ramp like, rather than a head, although at some points there is a clear billowing at the head of the land breeze, causing a more circular appearance. Figure 6 shows a PPI of the land breeze. In this image, a median high pass filter has been applied to the data in order to get a better picture of composition of the flow outside of the land breeze. Cellular structures with diameters of 0.5-1 km can be seen to the east of the land breeze in the convective onshore flow. Additional lidar imagery, including animations and wind vector fields can be found online at http://lidar.ssec.wisc.edu/pub_html/wisc97/index/dec/122197/index.htm.

4.2 *Model Output*

Several simulations of this particular date were run using the UW-NMS. Both of the two highlighted here consisted of six nested grids, with the second run having larger-sized domains for grids 4,5 and 6. Table 1 shows the statistics for both of these simulations. Simulation results show the presence of a land breeze circulation similar in structure to that seen in the lidar data. Figure 7 shows zonal images from the high-resolution domain, for three different altitudes, along with a cross section of the same domain. In this imagery, the land breeze is very noticeable, with westerly flow extending offshore, and easterly flow at offshore locations. From the vertical cross section, it is noticeable that this circulation is only around 50 m in depth, and that there is an updraft at the intersection of the two flows. Similar structures are present in the relative humidity and meridional (V) wind component fields. The vertical velocity output (figure 8) shows a very clear cellular structure in the flow coming across the lake. Additionally, there is a line of increased positive vertical velocity at the convergence zone between the land breeze and the prevailing flow.

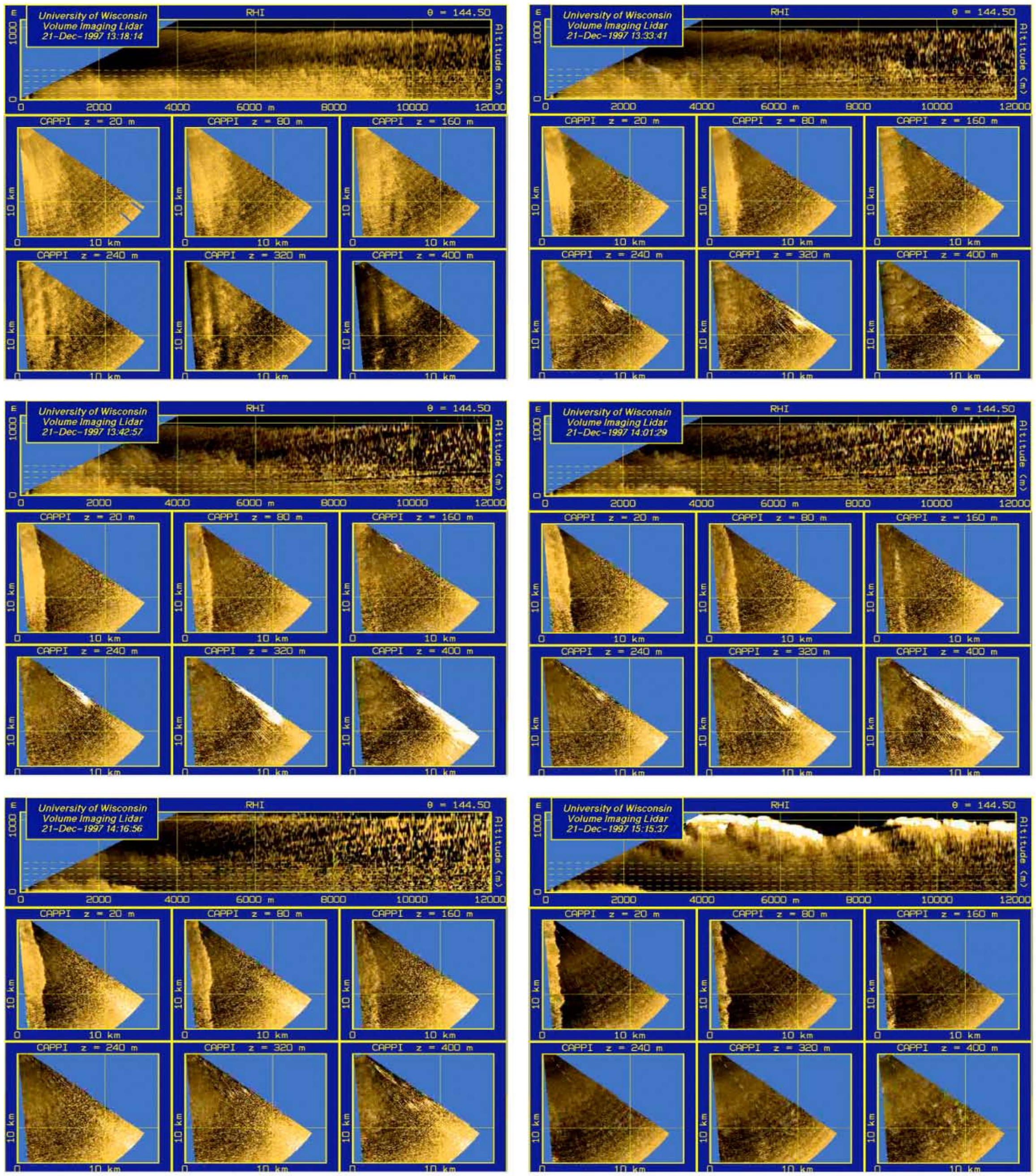

Figure 5: RHI Volume scans taken on December 21, 1997. The scans go from earliest (top left) to latest (bottom right).

GRID	1(A,B)	2 (A,B)	3 (A,B)	4A	5A	6A	4B	5B	6B
Hor. Points	65x65	77x77	52x52	132x132	182x182	182x182	197x157	452x362	502x502
Vert. Points	50	50	50	50	50	50	50	50	50
Hor. Resolution (m)	60000	12000	2400	480	160	32	480	160	32
Hor. Size (km)	3780x3780	900x900	120x120	62.4x62.4	28.8x28.8	5.76x5.76	93.6x74.4	72x57.6	16x16

Table 1: Domain properties of simulations ‘A’ and ‘B’.

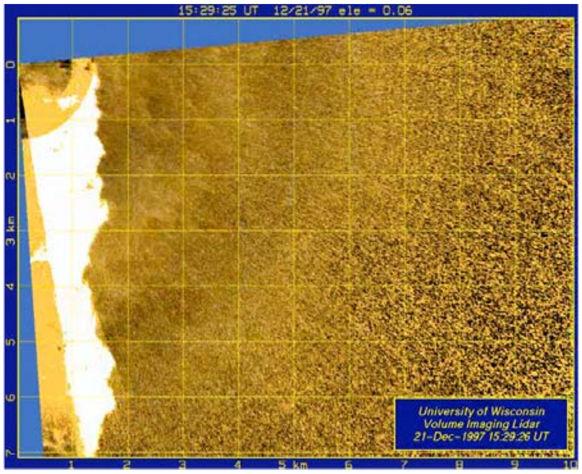

Figure 6: A PPI image enhanced using a high pass filter in order to observe structures in the onshore flow.

Figure 9 shows the virtual scattering parameter (Mayor, 2003) used in order to attempt direct comparison with the lidar imagery. In order to represent scattering in the model, two main variables are tracked. The first of these is a passive tracer, initialized with a value of 1 at the lowest 2 above ground grid boxes in the model run, and zero elsewhere. The flow then distributes the tracer, causing local minima and maxima in concentration. The other important variable looked at in the scattering parameter is the relative humidity. Several studies (Day and Malm, 2001; Fitzgerald and Hoppel, 1982) have shown the relationship between aerosol size/backscatter and relative humidity. For this study, we utilized the Fitzgerald data set of scattering vs. relative humidity in order to come up with the following relationship:

$$\alpha = -2.5 + \frac{8.4}{(100 - RH)^{0.2}} \quad (1)$$

where α is the scattering parameter, and RH is the relative humidity. The scattering parameter is then multiplied by the passive tracer, and finally, the log of the product of the two is taken in order to simulate the effect of the VIL's log amplifier. The horizontal scale of both of the figures is the width of the sixth domain, 16 kilometers. These images clearly show the land breeze, along with some Kelvin-Helmholtz type billows forming behind the head of the circulation. Also able to be investigated using this parameter is the structure of the

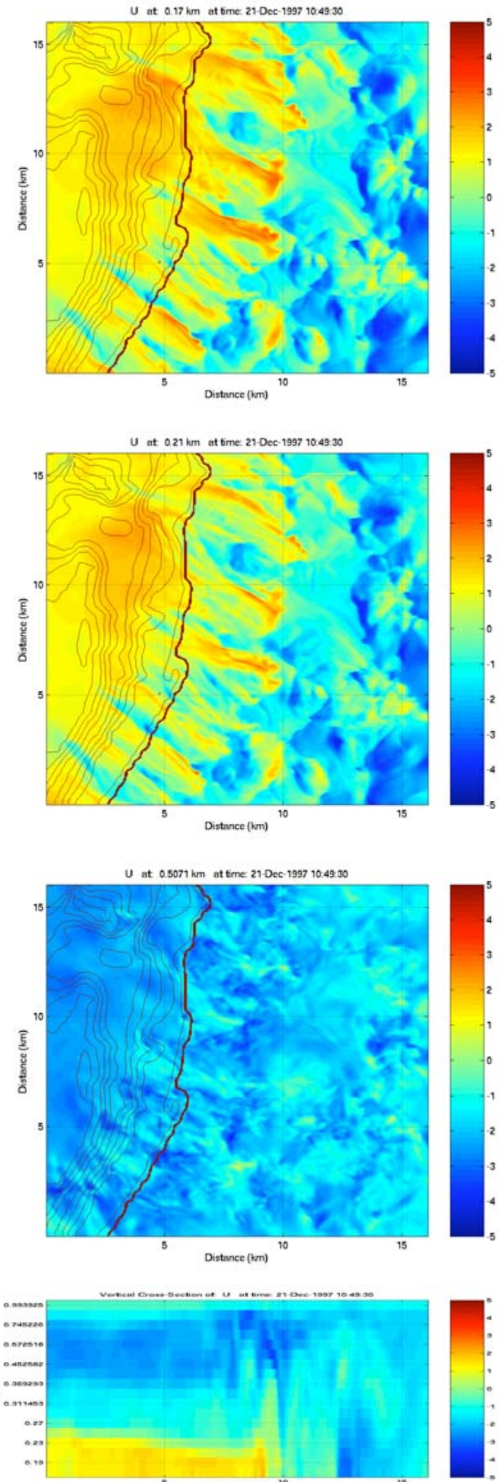

Figure 7: 6th grid model output of the zonal component of the flow velocity. The bottom image is a west (left) east (right) cross-section, while the top images are horizontal cross sections at the surface, 40 m, and 330 m, with topography contoured.

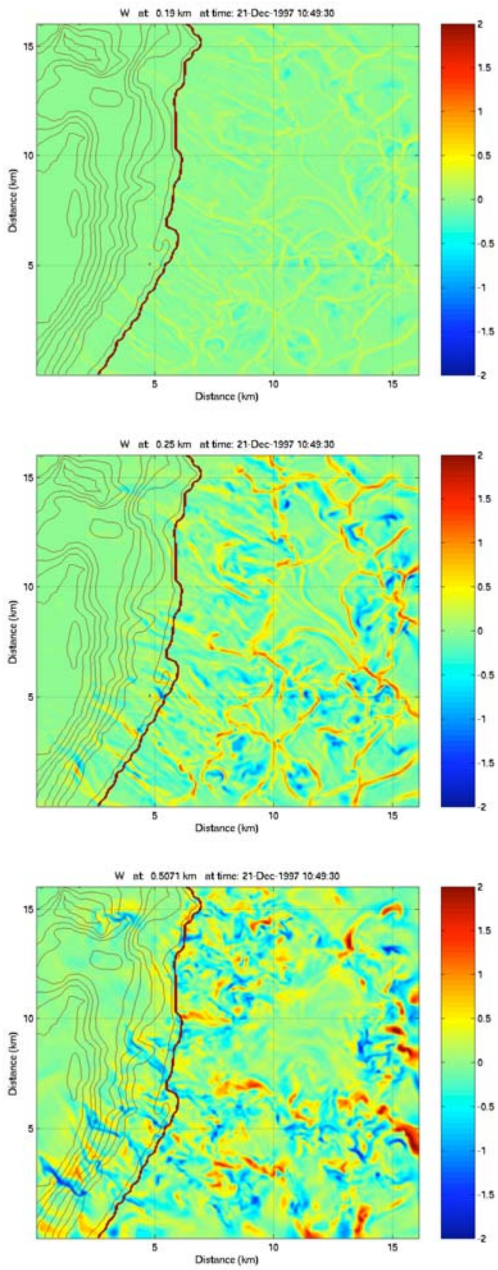

Figure 8: 6th grid model output of the vertical component of the flow velocity. The top images are looking down with topography contoured.

boundary layer, with high concentrations in scattering typically indicating an area of strong vertical velocity. The bottom half of figure 9 also gives insight into the structure of the convective, onshore flow coming across Lake Michigan and meeting the land breeze.

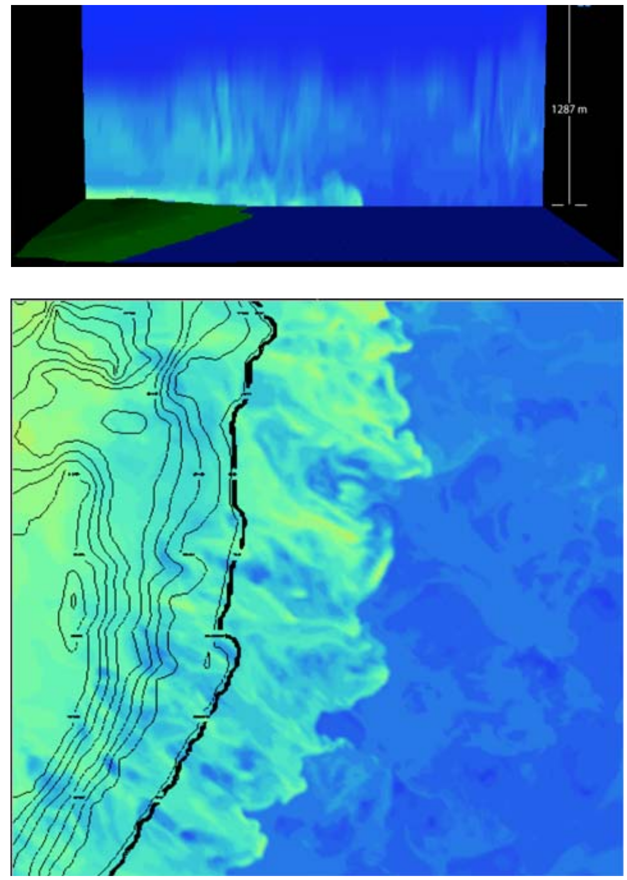

Figure 9: Model virtual scattering output. The horizontal extent of these domains is 16 km, and the vertical extent of the upper image is around 1290 m.

5. COMPARISON AND RESULTS

Comparison of the model output to the lidar data shows general agreement between the two. Frontal position seems to hold fairly steady in the model at around 3-4 km offshore, similar to the lidar position of 3 km or so. This is somewhat deceiving, because the lidar data shows several clear undulations in that position, with the front both moving towards and away from the shoreline at particular instances in time. Although some undulation is present in the model output, it is not as noticeable as in the lidar data.

The boundary layer structure surrounding the land breeze also appears to be in general agreement with that seen in the lidar data. The model output indicates that the boundary layer is approximately 800-900 m deep, which is very similar to the value derived by studying the scattering gradients of the lidar data. The structure of the flow coming across the lake to meet the land breeze shows cellular structures in both cases, with cell diameters around one kilometer.

The vertical extent of the land breeze seems to agree reasonably. In both the model and the lidar data, the land breeze itself is approximately 30-40 m deep, with the head showing a deeper structure of around 60-70 m. Again, this fluctuates some with time, particularly in the lidar observations.

The strength of both flows was analyzed as well. Again, there is general agreement between the observations taken at the NDBC site and the model output. Looking solely at the zonal wind speed, it may appear that the land breeze is somewhat weaker in the model output, but some of the wind speed is lost when the meridional component is not incorporated. The flow coming across the lake is more difficult to analyze, since no data was recorded at that position. Assuming the data from after the passage of the land breeze front over the NDBC site accurately represents the structure of that flow all along, it would appear as though the model flow is somewhat weaker than the actual flow. Additionally, the convective nature of this flow makes the horizontal winds somewhat more variable in direction.

One other important item for consideration is the temporal accuracy of the model results. Since this is a circulation forced mainly by large-scale events, there is some hope that the timing of major events (i.e. the retreat of the land breeze front over the shoreline) in the circulation can be captured. At the current time, this hypothesis has not been tested.

Accurate simulation of small-scale structures is an important step in the advancement of boundary layer forecasting. Given specific initial conditions, limited area models do a decent job of capturing flow features at these small scales. However, the inclusion of the large scale is often an integral part of correctly reproducing many of these structures, and therefore, efforts need to be in place to do so. The use of a model with nesting capabilities and the ability to handle both the large scale as well as fine scale phenomena is a large step in attempting to meet this need. In this study, a shallow land breeze was chosen as a small-scale event to attempt to simulate using the large scale as an initialization tool. Comparison with data recorded of the event by the UW-VIL shows general agreement with the model output. This agreement indicates that the utilization of a nesting model for simulation of small scale, boundary layer phenomena is a valid effort to aid in our understanding and forecasting of these features.

6. REFERENCES

Agee, E.M., M.L. Hart, 1990: Boundary Layer and Mesoscale Structure over Lake Michigan during a Wintertime Cold Air Outbreak. *Journal of the Atmospheric Sciences,* **47,** 2293-2316.

Alpert, P., J. Neumann, 1983: A Simulation of Lake Michigan's Winter Land Breeze on 7 November 1978. *Monthly Weather Review*, **111,** 1873-1881.

Atkins, N.T., et al., 1995: Observations of the Sea-Breeze Front during CaPE. Part II: Dual-Doppler and Aircraft Analysis. *Monthly Weather Review,* **123,** 944-969.

Ballentine, R.J.,1982: Numerical Simulation of Land-Breeze-Induced Snowbands Along the Western Shore of Lake Michigan. *Monthly Weather Review*, **110,** 1544-1553.

Day, D.E., W.C. Malm, 2001: Aerosol Light Scattering Measurements as a Function of Relative Humidity: A Comparison Between Measurements Made at Three Different Sites. *Atmospheric Environment,* **35,** 5169-5176.

Fast, J.D., L.S. Darby, 2004: An Evaluation of Mesoscale Model Predictions of Down-Valley and Canyon Flows and Their Consequences Using Doppler Lidar Measurements during VTMX 2000. *Journal of Applied Meteorology,* **43,** 420-436.

Fitzgerald, J.W., W.A. Hoppel, 1982: The Size and Scattering Coefficient of Urban Aerosol Particles at Washington, DC as a Function of Relative Humidity. *Journal of the Atmospheric Sciences,* **39,** 1838-1852.

Kristovich, D.A.R., et al., 2000: The Lake-Induced Convection Experiment and the Snowband Dynamics Project. *Bulletin of the American Meteorological Society,* **81,** 519-542.

Mayor, S.D., G.J. Tripoli, E.W. Eloranta, 2003: Evaluating Large-Eddy Simulations Using Volume Imaging Lidar Data. *Monthly Weather Review*, **131,** 1428-1452.

-----, 2001: Volume Imaging Lidar Observations and Large-Eddy Simulations of Convective Internal Boundary Layers (PhD Thesis: University of Wisconsin - Madison).

Moeng, C., P.P. Sullivan, 1994: A Comparison of Shear- and Buoyancy-Driven Planetary Boundary Layer Flows. *Journal of the Atmospheric Sciences*, **51,** 999-1022.

Ohara, T., I. Uno, S. Wakamatsu, 1989: Observed Structure of a Land Breeze Head in the Tokyo Metropolitan Area. *Journal of Applied Meteorology*, **28,** 693-704.

Sha, W., T. Kawamura, and H. Ueda, 1991: A Numerical Study on Sea/Land Breezes as a Gravity Current: Kelvin-Helmholtz Billows and Inland Penetration of the Sea-Breeze Front. *Journal of the Atmospheric Sciences*, **48,** 1649-1665.

Shafran, P.C., N.L. Seaman, G.A. Ganyo, 2000: Evaluation of Numerical Predictions of Boundary Layer Structure During the Lake Michigan Ozone Study. *Journal of Applied Meteorology,* **39,** 412-426.

Tripoli, G.J., 1992: A Non-Hydrostatic Mesoscale Model Designed to Simulate Scale Interaction. *Monthly Weather Review,* **120,** 1342-1359.

Winstead, N.S., 2000: Shallow Great Lake-Scale Atmospheric Thermal Circulation Imaged by Synthetic Aperture Radar. *Monthly Weather Review,* **128,** 3654-3663.